
 BULLETIN DE L'ASSOCIATION MINÉRALOGIQUE DU CANADA

THE CANADIAN MINERALOGIST

 JOURNAL OF THE MINERALOGICAL ASSOCIATION OF CANADA

Volume 41

August 2003

Part 4

The Canadian Mineralogist
Vol. 41, pp. 833-842 (2003)

SI-DEFICIENT, OH-SUBSTITUTED, BORON-BEARING VESUVIANITE FROM THE WILUY RIVER, YAKUTIA, RUSSIA

EVGENY V. GALUSKIN[§] AND IRINA O. GALUSKINA[§]

*Faculty of Earth Sciences, Department of Geochemistry, Mineralogy and Petrography,
University of Silesia, Będzińska 60, 41-200 Sosnowiec, Poland*

MACIEJ SITARZ

*Department of Material Sciences and Ceramics, University of Mining and Metallurgy, al. Mickiewicza 30,
Cracow, 30-059, Poland*

KATARZYNA STADNICKA

Faculty of Chemistry, Jagellonian University, Ingardena 3, Cracow, 30-060, Poland

ABSTRACT

A low-temperature, Si-deficient variety of vesuvianite occurs in porous tetrahedral "achtarandite" pseudomorphs consisting of hibschite, along the banks of the Wiluy River, Yakutia, Russia, the type locality of grossular and wiluite. The $(\text{H}_4\text{O}_4)^{4-}$ -for- $(\text{SiO}_4)^{4-}$ hydrogarnet-type substitution is evident in the vesuvianite, a substitution that allows it to be considered an analogue of hibschite. This variety of vesuvianite belongs to a new series in the vesuvianite group, as expressed by the formula $X_{19}Y_{13}T_{0-5}(\text{Si}_2\text{O}_7)_4(\text{SiO}_4)_{10-x}(\text{OH})_{4x}W_{10}$. The filling of the X, Y, and T positions in this Si-deficient vesuvianite, where x varies from 0.67 to 2.89, is analogous to that in vesuvianite and wiluite. The Si-deficient vesuvianite is characterized by increased unit-cell parameters, *a* 15.688(3), *c* 11.860(3) Å and by lower indices of refraction, ε 1.691(1), ω 1.668(1). In the OH-region, the FTIR and Raman spectra differ sharply from those of low-temperature vesuvianite from rodingites, but are similar to the spectra of hibschite. A line near 3620 cm^{-1} indicates that the substitution occurs only in the isolated tetrahedra. More than 25% of these can be substituted by (H_4O_4) . Contents of boron up to 2.48 *apfu* were detected in the Si-deficient vesuvianite. The vesuvianite formed during the hydration (serpentinization and rodingitization) of early, high-temperature skarns.

Keywords: Si-deficient vesuvianite, hydrogarnet-type substitution, boron, wiluite, infrared spectra, Raman spectra, electron-microprobe data, unit-cell parameters, Wiluy River, Russia.

SOMMAIRE

Une variété de vésuvianite déficitaire en Si, formée à basse température, fait partie d'un amas tétraédrique de hibschite formé par pseudomorphose ("achtarandite") le long des rives de la rivière Wiluy, en Yakoutie, Russie, la localité-type du grossulaire et de la wiluite. La substitution de $(\text{H}_4\text{O}_4)^{4-}$ au $(\text{SiO}_4)^{4-}$, comme c'est le cas dans un hydrogrenat, se manifeste donc dans la

[§] E-mail address: galuskin@us.edu.pl, irina@wnoz.us.edu.pl

vésuvianite, et mène à ce que l'on peut considérer comme un analogue de la hibschite. Cette variété de vésuvianite fait partie d'une nouvelle série du groupe de la vésuvianite, comme l'exprime la formule $X_{19}Y_{13}T_{0-5}(Si_2O_7)_4(SiO_4)_{10-x}(OH)_4W_{10}$. Le schéma utilisé pour remplir les sites X, Y, et T dans cette vésuvianite déficiente en Si, dans laquelle x varie de 0.67 à 2.89, est analogue à celui qui régit la vésuvianite et la wiluite. La vésuvianite déficiente en Si fait preuve d'une augmentation en paramètres réticulaires, a 15.688(3), c 11.860(3) Å, et d'une diminution des indices de réfraction, ε 1.691(1), ω 1.668(1). Dans la région où se trouvent les bandes OH, les spectres d'absorption infrarouge (avec transformation de Fourier) et de Raman diffèrent de façon marquée de ceux de la vésuvianite de basse température provenant des rodingites, mais ressemble à ceux de la hibschite. Une bande située près de 3620 cm^{-1} indiquerait que la substitution n'implique que les tétraèdres isolés. Plus de 25% de ceux-ci semblent remplacés par des agencements (H_4O_4). Des teneurs en bore atteignant jusqu'à 2.48 atomes par unité formulaire sont signalées dans la vésuvianite déficiente en Si. Cet exemple se serait formé lors d'une déshydratation (serpentinisation et rodingitisation) d'un skarn de haute température.

(Traduit par la Rédaction)

Mots-clés: vésuvianite déficiente en Si, substitution de type hydrogrenat, bore, wiluite, spectres infrarouges, spectres de Raman, données de microsonde électronique, paramètres réticulaires, rivière Wiluy, Russie.

INTRODUCTION

The common simplified formula of vesuvianite-group minerals is $X_{19}Y_{13}T_{0-5}(Z_2O_7)_4(ZO_4)_{10}W_{10}$. The X position is usually occupied by Ca, Y by Al, Mg, Fe^{3+} , Fe^{2+} , Mn^{2+} , and Ti, T by B and Al, Z by Si, and W by O, OH, F, and Cl. The boron-dominant structural analogue of vesuvianite, wiluite, has more than 2.5 of B atoms per formula unit (*apfu*) at the T position (Groat *et al.* 1998). The similarity of both vesuvianite and grossular in terms of structure and composition (Allen & Burnham 1992), as well as the common association of vesuvianite with hydrogrossular, suggest the possibility of a $(H_4O_4)^{4-}$ for $(SiO_4)^{4-}$ hydrogarnet-type substitution in vesuvianite. However, numerous investigations of vesuvianite from various environments have failed to provide any support for a hydrogarnet-type substitution (Groat *et al.* 1992, Fitzgerald *et al.* 1992, Lager *et al.* 1999).

Recently, Armbruster & Gnos (2000) discovered vacancies at the tetrahedral sites in low-temperature Mn-enriched vesuvianite from South Africa, which points to the possibility of the $(H_4O_4)^{4-}$ for $(SiO_4)^{4-}$ substitution. Contents of Si in these samples fluctuate slightly below the ideal 18 *apfu*, which indicates a low degree of substitution of the Si tetrahedra.

During our investigation of the vesuvianite-wiluite series of minerals from the Wiluy occurrence, along the banks of the Wiluy River, in Yakutia, split crystals and spherulitic arrays, some as large as 200 μm , were discovered within "achtarandite"-sponge pseudomorphs of hibschite after a wadalite-like phase (Galuskina *et al.* 1998, Galuskin & Galuskina 2002). These were found to be Si-deficient vesuvianite displaying an apparently considerable degree of substitution of $(SiO_4)^{4-}$ by $(H_4O_4)^{4-}$ (Galuskin *et al.* 2002). The vesuvianite-like phase forming a tight intergrowth with hydrogrossular in the alteration products of gehlenite probably also consist of Si-deficient vesuvianite. However, such material has not been investigated sufficiently thoroughly to draw a definitive conclusion (Henmi *et al.* 1994).

METHODS OF INVESTIGATION

The optical properties of the vesuvianite were investigated in thin sections and immersion preparations with the aid of a polarizing microscope. The morphology of the vesuvianite was studied using electron microscopes JSM-35C [(high vacuum (HV))] and FEI/Philips XL30 with EDS (EDAX) [HV and low vacuum (LV)]. Secondary electron [SE (HV)] and back-scattered electron [BSE (HV and LV, 0.3 Torr)] detectors were used to obtain images of the vesuvianite. During work in the LV regime, non-coated samples were used.

Electron-microprobe analyses were made using a CAMECA SX-100 instrument (Warsaw), taking into account the recommendations of McGee & Anovitz (1996) concerning the monitoring of boron. Measurements of the main components were performed at 15 kV and 20 nA for 20 seconds, using natural standards. Concentrations of F and B were measured at 5 kV and 100 nA for 50–100 seconds at each point. In measuring the concentration of boron, a danburite standard with control measurements from external standards (danburite, wiluite and boron-free marialite) was used.

The unit-cell parameters were calculated using the X'Pert Plus program on the basis of a powder X-ray pattern obtained using a Philips PW3710 diffractometer under the following conditions: 40 kV, 30 mA, 0.02° step, 35 seconds measurement-time per point. Following the standard method, the infrared spectrum of vesuvianite was also investigated, in KBr pellets at room temperature (resolution 4 cm^{-1}) and at 20 K (resolution 8 cm^{-1}) using a FTIR Digilab 60V (BioRad) spectrometer.

A sample of Si-deficient vesuvianite was analyzed on a Dilor Micro Raman spectrometer with a 514.5 nm argon ion laser. With this instrument, one focuses the size of the laser beam to about 5 μm on the surface of the sample. Raman spectra of vesuvianite-group phases from rodingites from the Urals, here given for comparison, have been collected using a FTS 6000 Bio-Rad spectrometer with Raman section (with Nd:YAG Spec-

tra Physics T10 106 4c laser) with a resolution of 4 cm^{-1} and 30,000 scans. The laser power was maintained at 200 mW on the sample.

MORPHOLOGY AND COMPOSITION OF SI-DEFICIENT VESUVIANITE

Light-cream spherulites and split crystals of Si-deficient vesuvianite with a characteristic nacreous luster were found inside “achtarandite” pseudomorphs (Fig. 1). These define compact intergrowths with a chlorite-group mineral and hibschite (Fig. 2). Sheaf-like crystals of vesuvianite are bounded by the $\{100\}$ and $\{101\}$ faces (Figs. 1a, b). The $\{001\}$ pinacoid faces, as main crystallographic form, appear on subindividuals of spherulites (Fig. 1c). The spherulites consist of flat subindividuals elongate parallel to the Z axis (Figs. 1d, 2) and possess an increased porosity. Both morphological forms of the Si-deficient vesuvianite developed as a

result of a splitting of the $\{100\}$ prism faces by an “autodeformation mechanism” connected with sectoral heterometry (Punin 2000, Galuskin *et al.* 2001).

The composition of the Si-deficient vesuvianite is close to that of vesuvianite from rodingites (*e.g.*, Groat *et al.* 1992, Fitzgerald *et al.* 1992). Si-deficient vesuvianite is characterized by a low content of Mg, Ti and Fe and a higher level of Al. This composition contrasts with that of the high-temperature wiluite associated with Si-deficient vesuvianite (Table 1, Fig. 3). There is a considerable variation in the contents of cations incorporated in the Y position, with a tendency for increasing Fe contents toward the margin of the spherulites (Fig. 3, Table 1).

Several zones, with a homogeneous structure in which aluminum is enriched, are significant. In these, the sum of the cations at the Y position is slightly more than 13 *apfu* (Fig. 2c, Table 1, anal. 3). This excess serves as evidence of limited replacement of Al for Si

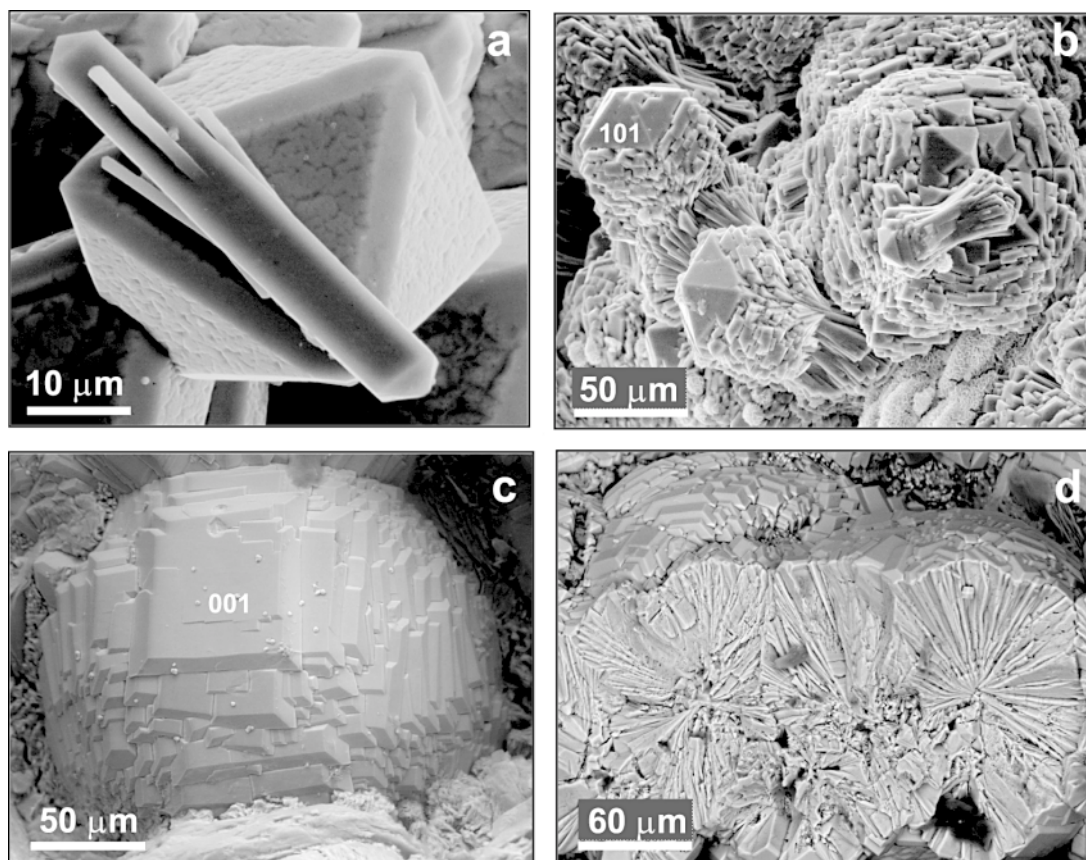


FIG. 1. Morphology of Si-deficient vesuvianite, SEM: a Split $\{100\}+\{101\}$ crystal on the $\{111\} + \{110\}$ crystal of hibschite, SE. b Sheaf-like $\{100\}+\{101\}$ crystals, SE. c Spherulites terminated by the $\{001\}$, $\{100\}$, $\{101\}$ faces, BSE (LV). d Radial structure of spherulite, BSE (LV).

and of occupancy of a small part of the Al at the $T(1)$ and $T(2)$ positions (Groat *et al.* 1994a). In general, the sum of cations incorporated at the Y position in vesuvianite is close to 13 *apfu* (Table 1), which indicates that the Al-for-Si substitution does not play a significant role.

The principal characteristic of the Wiluy River vesuvianite, which sets it apart from all other known samples of vesuvianite, is its low content of Si, near 15–16 *apfu* (Table 1, Fig. 4a). This feature demonstrates the considerable role of the $(O_4H_4)^+$ for $(SiO_4)^+$ substitution in Si-deficient vesuvianite from the Wiluy River, in analogy with hydrogrossular (Rinaldi & Passaglia 1989). In addition, thin late zones with increased contents of OH groups that exceed maximum possible contents of the OH groups at the W positions,

i.e., 9 *apfu*, are noted on crystals of wiluite and boron-rich vesuvianite (Fig. 4a, Galuskin *et al.*, in prep.).

No correlation is observed between amounts of Si and OH in wiluite with low contents of OH groups (Fig. 4a), but a negative correlation between B and OH occupying incompatible positions in the wiluite structure is plainly visible (Fig. 4b). The average content of boron in Si-deficient vesuvianite is lower than that in wiluite ($B > 2.5$ *apfu*) and usually does not exceed 2 *apfu* of B although, in rare cases, the content of boron exceeds 2.48 *apfu* (Fig. 4b, Table 1). It is likely that boron in Si-deficient vesuvianite occupies the $T(1)$ and $T(2)$ positions in the structure, as in boron-bearing vesuvianite and wiluite (Groat *et al.* 1994b, 1996, 1998). There is a negative correlation between amounts of Si and OH (Fig. 4a) in Si-deficient vesuvianite, with numbers of

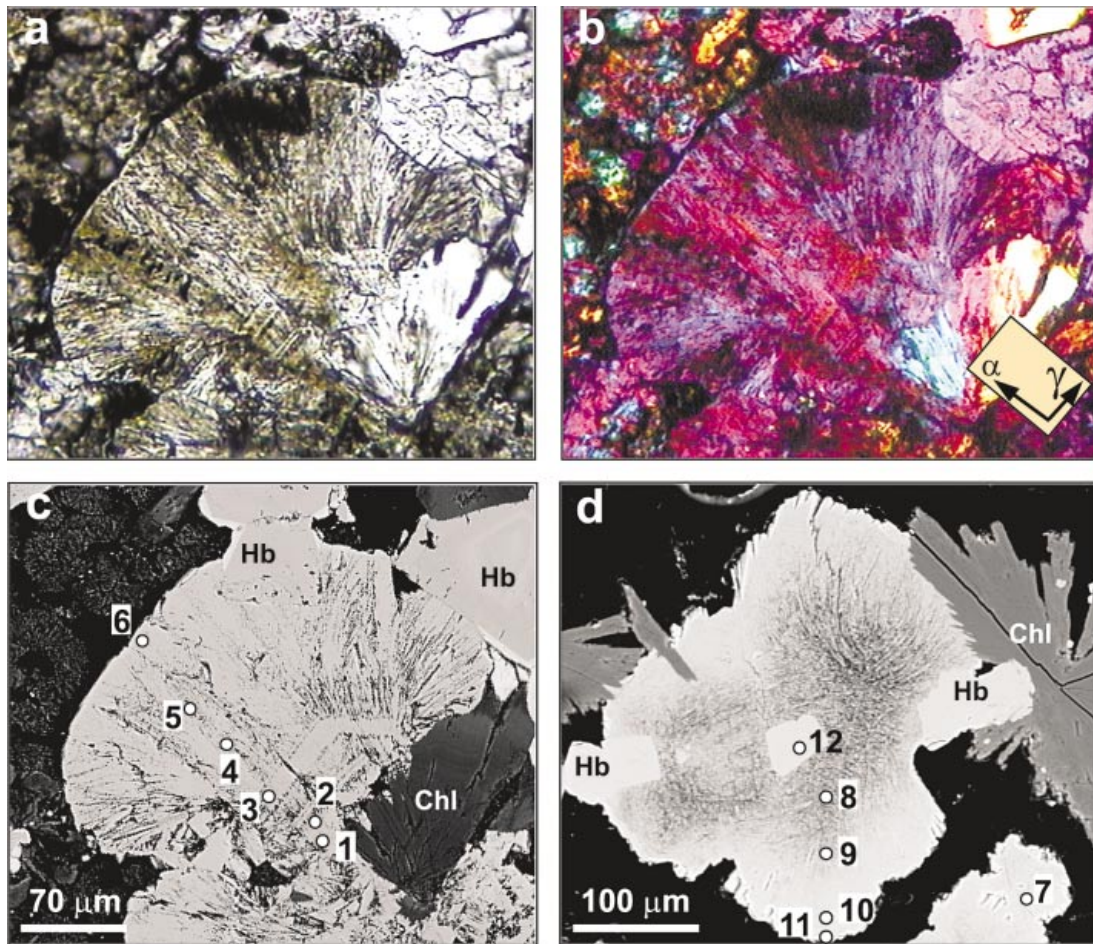


FIG. 2. Cross-section of split forms of Si-deficient vesuvianite. a–c Spherulite: transmitted light at parallel nicols (a) and crossed nicols with gypsum compensator (b) and BSE image (c), with sites of electron-microprobe analyses indicated (Table 1). d Sheaf-like crystals, BSE image with marked points of analyses (Table 1). Chl chlorite, Hb hibschite.

OH groups exceeding maximum possible numbers at the *W* position (taking in account isomorphism with other anions), which corroborates the occurrence of isomorphous $(\text{O}_4\text{H}_4)^{4-}$ for $(\text{SiO}_4)^{4-}$ substitution, as in hydrogarnet. There is a common tendency for increasing Si contents toward the margins of aggregates of Si-deficient vesuvianite (Table 1). Similar degrees of hydration of hibschite and Si-deficient vesuvianite are evident where they occur in association (Table 1, Galuskina *et al.* 2001).

Minerals of the hibschite–katoite series have increased unit-cell parameters, which reflect increasing Z–O and Ca–O interatomic distances (Lager *et al.* 1989). Hydrogarnet-group minerals also have lower indices of refraction than grossular. They are characterized by the appearance of bands near 3600–3620 and 3660 cm^{-1} in

the region of OH-stretching vibrations, which is indicative of the replacement of part of the Si in the tetrahedra by H (Żabiński 1965, Passaglia & Rinaldi 1984, Rinaldi & Passaglia 1989, Rossman & Aines 1991, Galuskina *et al.* 2001).

The Si-deficient vesuvianite from the Wiluy River is differentiated from typical vesuvianite by increased unit-cell parameters: a 15.688(3), c 11.860(3) Å. In the vesuvianite group, only in metamict vesuvianite do both parameters increase, whereas wiluite is characterized by an increased a parameter and a decreased c parameter (Groat *et al.* 1992).

The selection of a sample for single-crystal X-ray investigation was a major problem because all crystals have a domain and fibrous structure and a high porosity. Only in one case did we obtain diffraction data for a

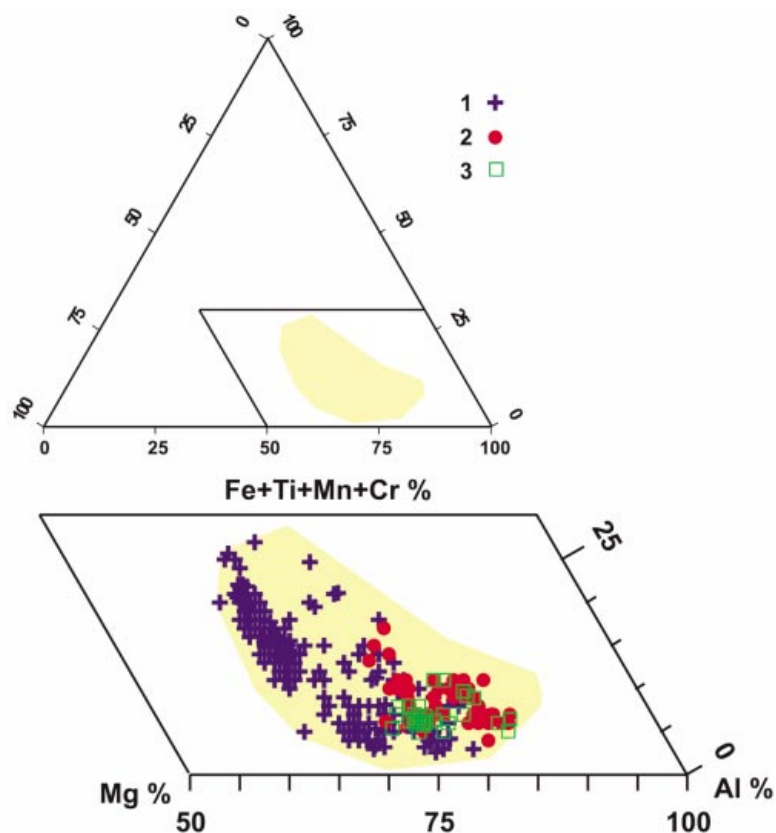


FIG. 3. Compositions of Si-deficient vesuvianite on the Al – (Fe + Ti + Mn + Cr) – Mg diagram (Y-type cations). Field of composition of the vesuvianite – wiluite series from the Wiluy occurrence is shown in yellow (Galuskin *et al.*, in prep.). 1 Large “classic” crystals of wiluite, 2 spherulites, and 3 sheaf-like crystals.

TABLE 1. CHEMICAL COMPOSITION (WT. %) AND DEGREE OF HYDRATION (*K*, %) OF SI-DEFICIENT VESUVIANITE, WILUITE AND HIBSCHITE

| | 1 | 2 | 3 | 4 | 5 | 6 | 7 | 8 | 9 | 10 | 11 | 12 | 13 |
|--|-------|-------|-------|-------|-------|-------|-------|-------|--------|-------|-------|-------------------|--------------------|
| SiO ₂ | 32.65 | 32.31 | 32.57 | 32.03 | 32.06 | 34.01 | 33.29 | 32.78 | 34.13 | 32.94 | 35.98 | 34.69 | 35.25 |
| TiO ₂ | 0.11 | 0.10 | 0.02 | 0.02 | 0.07 | 0.03 | 0.08 | 0.08 | 0.06 | 0.02 | 0.02 | 0.02 | 1.08 |
| Al ₂ O ₃ | 16.83 | 17.25 | 18.05 | 15.87 | 15.68 | 16.25 | 16.19 | 15.82 | 16.04 | 18.44 | 16.80 | 20.60 | 10.07 |
| B ₂ O ₃ | 2.93 | 1.46 | 0.70 | 0.65 | 0.52 | 0.65 | 2.47 | 2.94 | 2.45 | 1.71 | 1.43 | 0.52 | 3.22 |
| Fe ₂ O ₃ * | 2.01 | 1.80 | 1.88 | 2.43 | 3.23 | 3.24 | 1.94 | 2.00 | 1.91 | 1.71 | 3.44 | 1.66 | 5.76 |
| MgO | 3.57 | 3.19 | 3.02 | 3.85 | 3.74 | 3.66 | 4.19 | 4.24 | 4.42 | 2.83 | 3.22 | 0.90 | 6.16 |
| CaO | 36.71 | 36.69 | 36.57 | 36.95 | 36.89 | 36.41 | 36.72 | 36.35 | 37.16 | 36.73 | 36.31 | 37.85 | 35.39 |
| MnO | 0.22 | 0.60 | 0.44 | 0.52 | 0.41 | 0.31 | 0.14 | 0.10 | 0.10 | 0.09 | 0.05 | 0.08 | 0.09 |
| H ₂ O** | 3.16 | 4.43 | 4.44 | 5.69 | 5.59 | 3.62 | 3.10 | 2.90 | 3.07 | 2.87 | 1.87 | 3.24 | 1.05 |
| Cl | 0.63 | 0.48 | 0.45 | 0.45 | 0.47 | 0.43 | 0.44 | 0.36 | 0.40 | 0.40 | 0.23 | n.d. | n.d. |
| F | 0.33 | 0.38 | 0.40 | 0.50 | 0.53 | 0.57 | 0.61 | 0.57 | 0.68 | 0.40 | 0.08 | 0.22 | 0.13 |
| SO ₃ | n.a. | n.a. | n.a. | n.a. | n.a. | n.a. | 0.11 | 0.06 | 0.05 | 0.05 | n.a. | n.a. | n.a. |
| -O=F+Cl | 0.28 | 0.27 | 0.27 | 0.31 | 0.33 | 0.34 | 0.36 | 0.32 | 0.38 | 0.26 | 0.12 | 0.09 | 0.06 |
| Total | 98.87 | 98.42 | 98.27 | 98.65 | 98.86 | 98.84 | 98.92 | 97.89 | 100.10 | 98.86 | 99.31 | 99.69 | 98.14 ^x |
| Calculated on charge 156-(Cl+F) and normalized on 19Ca | | | | | | | | | | | | | |
| Ca/X | 19 | 19 | 19 | 19 | 19 | 19 | 19 | 19 | 19 | 19 | 19 | 18 ^{xxx} | 19 |
| Ti ⁴⁺ | 0.04 | 0.04 | 0.01 | 0.01 | 0.03 | 0.01 | 0.03 | 0.03 | 0.02 | 0.01 | 0.01 | 0.01 | 0.41 |
| Al | 9.58 | 9.82 | 10.31 | 8.98 | 8.88 | 9.32 | 9.21 | 9.10 | 9.02 | 10.49 | 9.67 | 10.78 | 5.95 |
| Fe ³⁺ | 0.73 | 0.65 | 0.68 | 0.88 | 1.17 | 1.19 | 0.71 | 0.73 | 0.69 | 0.62 | 1.26 | 0.55 | 2.18 ^{xx} |
| Mg | 2.57 | 2.30 | 2.18 | 2.76 | 2.68 | 2.66 | 3.02 | 3.09 | 3.14 | 2.04 | 2.35 | 0.60 | 4.60 |
| Mn ²⁺ | 0.09 | 0.24 | 0.18 | 0.21 | 0.17 | 0.13 | 0.06 | 0.04 | 0.04 | 0.04 | 0.02 | 0.03 | 0.04 |
| Y | 13.01 | 13.05 | 13.37 | 12.83 | 12.93 | 13.31 | 13.03 | 12.99 | 12.91 | 13.20 | 13.31 | 12 | 13.17 |
| B/T | 2.44 | 1.22 | 0.59 | 0.54 | 0.43 | 0.54 | 2.06 | 2.48 | 2.02 | 2.19 | 1.20 | 0.40 | 2.78 |
| Si ⁴⁺ /Z | 15.77 | 15.61 | 15.79 | 15.37 | 15.41 | 16.56 | 16.07 | 15.99 | 16.28 | 15.90 | 17.58 | 15.40 | 17.66 |
| S ⁶⁺ | | | | | | | 0.04 | 0.02 | 0.02 | 0.02 | | | |
| OH | 10.17 | 14.28 | 14.36 | 18.22 | 17.91 | 11.75 | 10.05 | 9.44 | 9.80 | 9.27 | 6.09 | 9.60 | 3.50 |
| F | 0.50 | 0.58 | 0.61 | 0.76 | 0.81 | 0.89 | 0.93 | 0.88 | 1.03 | 0.62 | 0.35 | 0.31 | 0.21 |
| Cl | 0.52 | 0.39 | 0.37 | 0.36 | 0.38 | 0.35 | 0.36 | 0.30 | 0.32 | 0.33 | 0.07 | | |
| <i>K</i> , % | 22.3 | 23.9 | 22.1 | 26.3 | 25.9 | 14.4 | 18.9 | 19.9 | 17.0 | 20.8 | 4.2 | 14.4 | 3.4 |

1-6 - {100}+{001}+{101} spherulites of Si-deficient vesuvianite (Fig.2c), 7-11 {100}+{101} sheaf-like split crystal of Si-deficient vesuvianite (Fig. 2d), 12 - {110} hibschite (fig.2d), 13- late zone of {100} growth sector of wiluite crystal.

*- total iron as Fe₂O₃, **- water calculated by valence balance, ^x - in total 0.02 Cr₂O₃, ^{xx} - Fe³⁺+Cr³⁺, ^{xxx} - calculated on charge 144-F and normalized on 18 Ca, n.a. - not analyzed, n.d. - not detected, *K* - % of vacancies in isolated Z(1,2) tetrahedra [≈degree of hydration of SiO₄ tetrahedra (Rinaldi & Passaglia 1989)].

vesuvianite crystal of pinacoidal type ($0.22 \times 0.22 \times 0.15$ mm) with the crystal-chemical formula $\text{Ca}_{19}(\text{Al}_{9.02}\text{Mg}_{3.22}\text{Fe}^{3+}_{0.58}\text{Mn}^{2+}_{0.16}\text{Ti}^{4+}_{0.02})_{\Sigma 13}(\text{B}_{0.81}\text{Al}_{0.09})_{\Sigma 0.9}[(\text{SiO}_4)_{8.05}(\text{H}_4\text{O}_4)_{1.95}]_{\Sigma 10}[\text{Si}_2\text{O}_7]_4(\text{OH}_{7.18}\text{O}_{2.37}\text{F}_{0.36}\text{Cl}_{0.09})_{\Sigma 10}$ (Galuskin *et al.*, in prep.). A structure refinement of this vesuvianite ($P4/nnc$, $R1 = 6.36\%$) reveals a significant number of vacancies (~15%) in isolated Si-tetrahedra [Z(1,2)] and an increase in Z(1)–O atomic distances, up to 1.686 Å (Galuskin *et al.*, in prep.). This finding confirms our inference concerning a hydrogarnet-type substitution in Si-deficient vesuvianite.

Lower indices of refraction, $\varepsilon = 1.691(1)$, $\omega = 1.668(1)$, are typical of Si-deficient vesuvianite (for more ferrous varieties, see Table 1). The optic sign is variable, depending on which growth sectors of the vesuvianite faces participate in the formation of spherulites (Fig. 2b; Galuskin *et al.* 2001). The angle $2V$ could not be measured in the central part of spherulites because of the thin fibrous structure (Figs. 1d, 2a). A biaxial character is not evident in the thin optically negative part at the margin of the spherulites.

FTIR spectra of the OH-region of the Si-deficient vesuvianite differ sharply from spectra typical of low-temperature vesuvianite and display a similarity to the spectra of hibschite (Fig. 5). At room temperature, the position of absorption bands is not successfully defined on the spectra of the Si-deficient vesuvianite. Only a lower-temperature measurement at 20 K, following decomposition of the spectra using the method proposed by Handke *et al.* (1994), allows for the demarcation of a few absorption bands: 3618, 3534, 3442, 3351 and 3235 cm^{-1} . The 3618 cm^{-1} band is typical of hydrogarnet, and reflects the $(\text{H}_4\text{O}_4)^{4+}$ for $(\text{SiO}_4)^{4-}$ substitution (Rossman & Aines 1991). An analogous band is observed in the hibschite spectrum (Fig. 5, spectrum 3). The absence of a second absorption band near 3660 cm^{-1} , which is typical of katoite, indicates that $(\text{H}_4\text{O}_4)^{4+}$ groups are adjacent to $(\text{SiO}_4)^{4-}$ groups, and that there are no further $(\text{H}_4\text{O}_4)^{4+}$ groups in the vicinity (Rossman & Aines 1991). The similarity of the spectra of hibschite and the Si-deficient vesuvianite (Fig. 5) may indicate $(\text{H}_4\text{O}_4)^{4+}$ for $(\text{SiO}_4)^{4-}$ substitution only in the single tetrahedra Z(1,2), where their degree of hydration exceeds 25% (Table 1). Armbruster & Gnos (2000) noted the absence of replacement of Si by H in the $(\text{Si}_2\text{O}_7)^{6-}$ groups.

We note the presence of a band near 3631 cm^{-1} , close to the 3618 cm^{-1} band, in the spectrum of low-temperature olive-green vesuvianite from rodingite occurrences in the Urals [$\text{Ca}_{19}\text{Al}_9\text{Mg}_2\text{Fe}^{3+}_2\text{Si}_{18}\text{O}_{69}(\text{OH})_9$, a 15.533(1), c 11.831(1) Å]. The 3670 cm^{-1} band is not connected with the substitution $(\text{H}_4\text{O}_4)^{4+}$ for $(\text{SiO}_4)^{4-}$, but it is characteristic of the Y(3)–Y(2)–O(11)H(1) configuration (Fig. 5, spectrum 4). The 3631 cm^{-1} band is characteristic of the Al–Al–OH configuration, and the 3670 cm^{-1} band, of the Mg–Al–OH configuration (Groat *et al.* 1995). These bands are not evident in Si-deficient vesuvianite, probably because of the incorporation of F

at the O(11) position or of B at the T(1) position. The 3516 cm^{-1} band in the vesuvianite spectrum, and also a weak band near the 3534 cm^{-1} band in the spectrum of Si-deficient vesuvianite, are probably defined by the Fe^{3+} –Al–OH configuration (Groat *et al.* 1995). The positions and shapes of bands near 3442 (Si-deficient vesuvianite), 3431 (hibschite) and 3423 cm^{-1} (vesuvianite) indicate the presence of molecules of H_2O (Fig. 5).

Vesuvianite from the rodingite shows a pronounced band near 3155 cm^{-1} (Fig. 5, spectrum 4); it is characteristic of low-temperature, ordered vesuvianite, with a symmetry lower than $P4/nnc$, and is defined by the local O(10)H(2)[–] ... O(10)^{2–} configuration (Žabiński & Paluszkiwicz 1994, Groat *et al.* 1995). Si-deficient vesuvianite does not possess an analogous band, but we do see very weak broad bands higher than 3200 cm^{-1} , which may indicate a low degree of order in the vicinity of the O(10) position. Boron atoms at the T(2) position, and F and Cl at the O(10) position, will influence the character of spectra and lead to reduction of the intensity of the OH-band.

Sharp distinctions between vesuvianite from the Urals rodingites and the Si-deficient vesuvianite from Wiluy River are observed in the OH region on Raman spectra (Fig. 6). The intense band near 3622 cm^{-1} is analogous to the 3618 cm^{-1} band on the FTIR spectra (Fig. 5); it is noted in spectra of hydrogrossular and points to a hydrogarnet type of substitution in the isolated tetrahedra (Arredondo & Rossman 2002). This band is absent in the spectra of vesuvianite from the rodingite, but there is a broad band near 3150–3200 cm^{-1} that appears to be analogous to a similar band defined on FTIR spectra that is connected with the O(10)H(2)[–] ... O(10)^{2–} configuration.

The crystal-chemical formula of highly OH-substituted, Si-deficient vesuvianite can be presented as $X_{19}Y_{13}T_{0-2.5}(\text{Si}_2\text{O}_7)_4(\text{SiO}_4)_{10-x}(\text{OH})_{4x}(\text{OH},\text{O},\text{F},\text{Cl})_{10}$, where the occupants of the X, Y, and T positions are analogous to those in vesuvianite and wiluite, and $0.67 < x < 2.89$ for Wiluy Si-deficient vesuvianite. In this series, only a phase with $x > 5$ could be considered as a new mineral species (“hydrovesuvianite”), according to the rule of CNMMN IMA (Nickel & Grice 1998). It is interesting that some compositions of Si-deficient vesuvianite are very close to the field of wiluite (Fig. 4, Groat *et al.* 1998), which may indicate the presence in nature of Si-deficient wiluite (“hydrowiluite”).

A predominance of oxygen at the W position, for example $\text{Ca}_{19}\text{Al}_{9.21}(\text{Mg}_{3.02}\text{Fe}^{3+}_{0.71}\text{Mn}^{2+}_{0.06}\text{Ti}_{0.03})_{\Sigma 13.03}\text{B}_{2.06}(\text{Si}_2\text{O}_7)_4(\text{SiO}_4)_{8.11}(\text{OH})_{7.56}(\text{O}_{6.22}\text{OH}_{2.49}\text{F}_{0.93}\text{Cl}_{0.36})_{\Sigma 10}$ (anal. 7, Table 1), is noted in Si-deficient vesuvianite with high contents of boron. A predominance of oxygen at the W position is characteristic of wiluite, but not of typical vesuvianite from various environments (Fitzgerald *et al.* 1992, Groat *et al.* 1992, 1998).

The formation of Si-deficient vesuvianite was a result of the hydration (serpentinization and rodingitization) of early high-temperature layered skarns

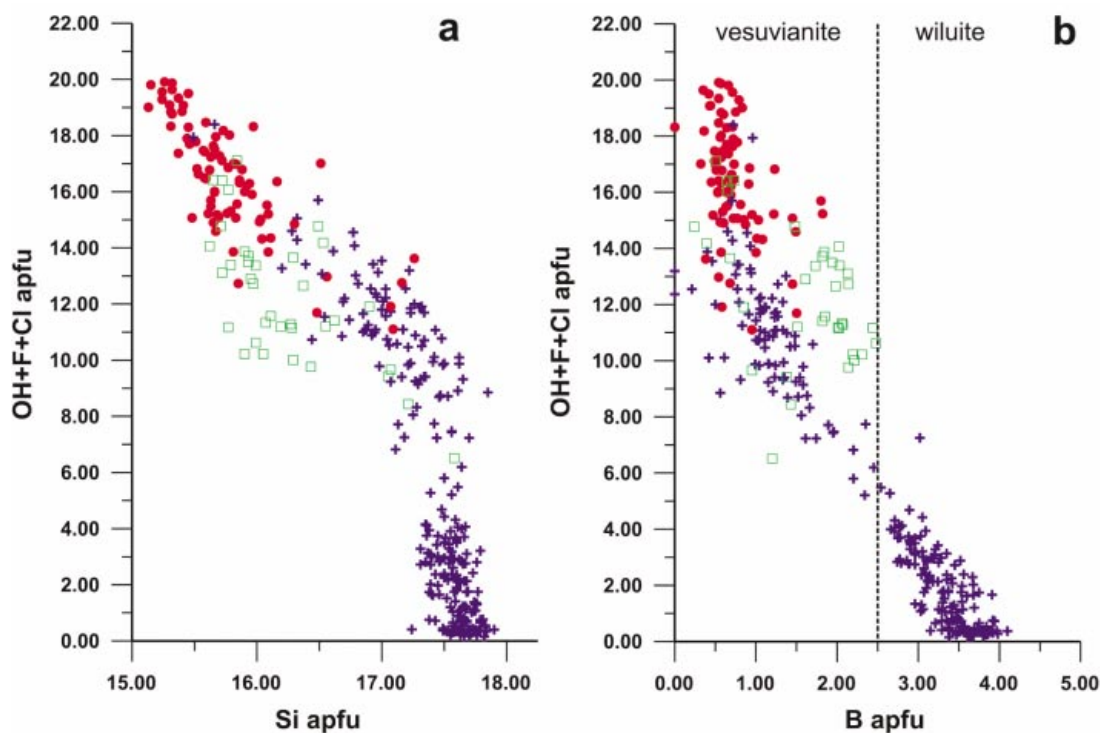


FIG. 4. Compositions of Si-deficient vesuvianite and wiluite in terms of $(OH + F + Cl) - Si$ (a) and $(OH + F + Cl) - B$ (b) diagrams. For explanation of symbols, see Figure 3.

associated with magmatic rocks of Siberian Trap Formation on the Wiluy River (Galuskina *et al.* 1998, 2001). Crystallization of Si-deficient vesuvianite and of hibschite progressed under non-equilibrium conditions, a fact reflected in their morphology. The conditions under which crystallization occurred are characterized by high Al/Si and Ca/Si in the mineral-forming solutions, high $P(H_2O)$ and $300 < T < 350^\circ C$ (Galuskina *et al.* 2001).

ACKNOWLEDGEMENTS

We thank Prof. J.A. Mandarino, Prof. D.Yu. Pushcharovsky and Dr. J.D. Grice for discussions connected with the problems of vesuvianite-group nomenclature. We also thank Dr. P. Dzierzanowski (University of Warsaw) for technical assistance with the electron-microprobe analyses. We also thank Dr. Padhraig Kennan and Mr. David Gordon for their comments regarding English usage, and Dr. M. Gunter for editorial work. We thank Prof. T. Armbruster, Prof. L.A. Groat, an anonymous referee, and R.F. Martin for their constructive comments on this paper. Financial support for this project was provided by the Scientific Research

Fund of the University of Silesia under grant BW-22/2000 and "KBN" (Polish Committee for Research) grant 3P04D 03622.

REFERENCES

- ALLEN, F.M. & BURNHAM, C.W. (1992): A comprehensive structure-model for vesuvianite: symmetry variations and crystal growth. *Can. Mineral.* **30**, 1-18.
- ARMBRUSTER, T. & GNOS, E. (2000): Tetrahedral vacancies and cation ordering in low-temperature Mn-bearing vesuvianites: indication of hydrogarnet-like substitution. *Am. Mineral.* **85**, 570-577.
- ARREDONDO, E.H. & ROSSMAN, G.R. (2002): Feasibility of determining the quantitative OH content of garnets with Raman spectroscopy. *Am. Mineral.* **87**, 307-311.
- FITZGERALD, S., LEAVENS, P.B. & NELEN, J.A. (1992): Chemical variation in vesuvianite. *Mineral. Petrol.* **46**, 163-178.
- GALUSKIN, E. & GALUSKINA, I. (2002): Achtarandite – sponge hibschite pseudomorph after wadalite-like phase: internal morphology and mechanism of formation. *Neues Jahrb. Mineral., Abh.* **178**, 63-74.

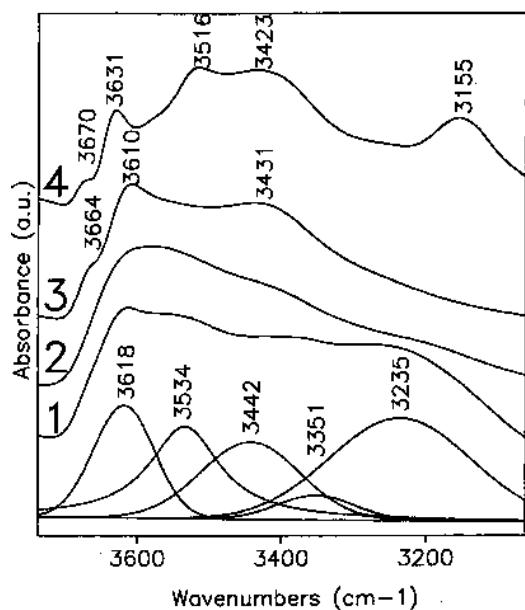


FIG. 5. IR spectra. 1, 2 Si-deficient vesuvianite, 1 at 20 K, with results of fit shown at the bottom, 2 at room temperature conditions. 3 Spectrum of hibschite (Galuskina *et al.* 2001). 4 Spectrum of vesuvianite from rodingites (Urals).

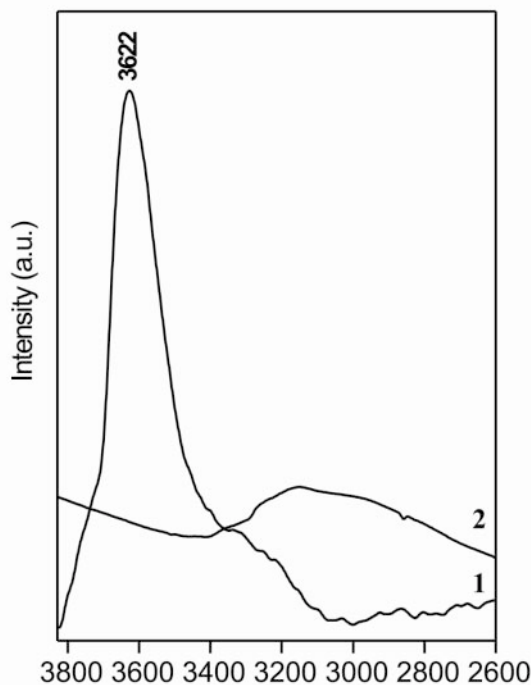


FIG. 6. Raman spectra of Si-deficient vesuvianite (1) and of vesuvianite of rodingites from Urals (2).

_____, _____ & SITARZ, M. (2001): The autodeformation mechanism of splitting of boron "hydrovesuvianite" crystals. *In* Symp. on Crystallogenes and Mineralogy (Saint Petersburg), 118 (abstr.).

_____, _____ & STADNICKA, K. (2002): High-hydrated Si-deficient vesuvianite ("hydrovesuvianite") from Yakutia, Russia. *Int. Mineral. Assoc., 18th Gen. Meeting (Edinburgh), Programme Abstr.*, 134.

GALUSKINA, I., GALUSKIN, E. & SITARZ, M. (1998): Atoll hydrogarnets and mechanism of the formation of achtarandite pseudomorphs. *Neues Jahrb. Mineral., Monatsh.*, 49-62.

_____, _____ & _____ (2001): Evolution of morphology and composition of hibschite, Wiluy River, Yakutia. *Neues Jahrb. Mineral., Monatsh.*, 49-66.

GROAT, L.A., HAWTHORNE, F.C. & ERCIT, T.S. (1992): The chemistry of vesuvianite. *Can. Mineral.* **30**, 19-48.

_____, _____ & _____ (1994a): Excess Y-group cations in the crystal structure of vesuvianite. *Can. Mineral.* **32**, 497-504.

_____, _____ & _____ (1994b): The incorporation of boron into the vesuvianite structure. *Can. Mineral.* **32**, 505-523.

_____, _____ & GRICE, J.D. (1998): Wiluite $\text{Ca}_{19}(\text{Al}, \text{Mg}, \text{Fe}, \text{Ti})_{13}(\text{B}, \text{Al}, \square)_5\text{Si}_{18}\text{O}_{68}(\text{O}, \text{OH})_{10}$, a new mineral species isostructural with vesuvianite, from the Sakha republic, Russian Federation. *Can. Mineral.* **36**, 1301-1304.

_____, _____, LAGER, G.A., SCHULTZ, A.J. & ERCIT, T.S. (1996): X-ray and neutron crystal-structure refinements of boron-bearing vesuvianite. *Can. Mineral.* **34**, 1059-1070.

_____, _____, ROSSMAN, G.R. & ERCIT, T.S. (1995): The infrared spectroscopy of vesuvianite in the OH region. *Can. Mineral.* **33**, 609-626.

HANDKE, M., MOZGAWA, M. & NOCUĆ, M. (1994): Specific features of the IR spectra of silicate glasses. *J. Molec. Struct.* **325**, 129.

HENMI, C., KUSACHI, I. & HENMI, K. (1994): Vesuvianite from Kushiro, Hiroshima Prefecture, Japan. *Int. Mineral. Assoc., 16th Gen. Meeting (Pisa), Programme Abstr.*, 172-173.

LAGER, G.A., ARMBRUSTER, T., ROTELLA, F.J. & ROSSMAN, G.R. (1989): OH substitution in garnets: X-ray and neutron diffraction, infrared, and geometric-modelling studies. *Am. Mineral.* **74**, 840-851.

- _____, XIE, QIANYEN, ROSS, F.K., ROSSMAN, G.R., ARMBRUSTER, T., ROTELLA, F.J. & SCHULTZ, A.J. (1999): Hydrogen-atom position in *P4/nnc* vesuvianite. *Can. Mineral.* **37**, 763-768.
- MCGEE, J.J. & ANOVITZ, L.M. (1996): Electron probe microanalysis of geological materials for boron. In *Boron: Mineralogy, Petrology and Geochemistry* (E.S. Grew & L.M. Anovitz, eds.). *Rev. Mineral.* **33**, 771-788.
- NICKEL, E.H. & GRICE J.D. (1998): The IMA commission on new minerals and mineral names: procedures and guidelines on mineral nomenclature, 1988. *Can. Mineral.* **36**, 913-926.
- PASSAGLIA, E. & RINALDI, R. (1984): Katoite, a new member of the $\text{Ca}_3\text{Al}_2(\text{SiO}_4)_3 - \text{Ca}_3\text{Al}_2(\text{OH})_{12}$ series and new nomenclature for the hydrogrossular group of minerals. *Bull. Minéral.* **107**, 605-618.
- PUNIN, YU.O. (2000): Role of the habit of crystals in formation of autodistortion defects. *Zap. Vser. Mineral. Obshchest.* **129**(6), 1-11 (in Russ.).
- RINALDI, R. & PASSAGLIA, E. (1989): Hibschite topotype: crystal chemical characterization. *Eur. J. Mineral.* **1**, 639-644.
- ROSSMAN, G.R. & AINES, R.D. (1991): The hydrous components in garnets: grossular-hydrogrossular. *Am. Mineral.* **76**, 1153-1164.
- ŻABIŃSKI, W. (1965): A study of minerals of the hydrogarnet group. *Bull. Cracow Acad. Mining Metall.* **38**(102), 1-91 (in Polish).
- _____ & PALUSZKIEWICZ, C. (1994): Infrared spectroscopic evidence of ordering in the vesuvianite structure. *Mineral. Polon.* **25**(1), 51-58.

Received December 2, 2002, revised manuscript accepted July 13, 2003.